Chem Soc Rev

TUTORIAL REVIEW

View Article Online
View Journal | View Issue

Cite this: *Chem. Soc. Rev.*, 2018, **47**, 5541

Semi-solid and solid frustrated Lewis pair catalysts

Yuanyuan Ma,[a] Sai Zhang,[a] Chun-Ran Chang,[a] Zheng-Qing Huang,[a] Johnny C. Ho[bc] and Yongquan Qu*[a]

Received 26th December 2017

DOI: 10.1039/c7cs00691h

rsc.li/chem-soc-rev

Recently discovered homogeneous frustrated Lewis pairs (FLPs) have attracted much attention for metal-free catalysis due to their promising potential for the activation of small molecules (*e.g.*, H_2, CO, CO_2, NO_x and many others). Hence, a wide range of these homogeneous FLPs have been extensively explored for many advanced organic syntheses, radical chemistry and polymerizations. In particular, these FLPs are efficiently utilized for the hydrogenation of various unsaturated substrates (*e.g.*, olefins, alkynes, esters and ketones). Inspired by the substantial progress in these homogeneous catalytic systems, heterogeneous FLP catalysts, including semi-solid and all-solid catalysts, have also emerged as an exciting and evolving field. In this review, we highlight the recent advances made in heterogeneous FLP-like catalysts and the strategies to construct tailorable interfacial FLP-like active sites on semi-solid and all-solid FLP catalysts. Challenges and outlook for the further development of these catalysts in synthetic chemistry will be discussed.

Key learning points
(1) Conceptual introduction of heterogeneous FLP catalysts.
(2) State-of-the-art of the major strategies for the construction of heterogeneous FLP catalysts.
(3) Recent progress in the design and synthesis of semi-solid and solid FLPs.
(4) Summary of the catalytic applications of the constructed heterogeneous FLP catalysts.
(5) Challenges and opportunities in the design and synthesis of heterogeneous FLP catalysts.

Introduction

In general, a frustrated Lewis pair (FLP) originates from the combination of a Lewis acid and a Lewis base that are sterically prevented from forming a classic Lewis acid–base adduct.[1–4] This unique formation of the FLP is usually dependent on the properly designed functional groups with the appropriate steric hindrance, not only inhibiting the direct adduction of the Lewis acid and base, but at the same time also preserving the essential interaction between the Lewis acid and base. These preserved Lewis acidic and basic features in a FLP would then enable its interaction with a third molecule, triggering the capability of the FLP for the activation of small molecules, such as H_2, CO_2, *etc.*[2–16] This distinctive dative Lewis acid–base configuration was discovered initially for stoichiometric reactivity and then extended for use as catalysts. In 2006, Douglas W. Stephan reported the first FLP example, *p*-$(Mes_2PH)C_6F_4(BH(C_6F_5)_2)$, which was demonstrated to deliver the reversible cleavage and liberation of H_2 at 25 °C and 150 °C, respectively (Scheme 1a).[17] Intermolecular $R_3P/B(C_6F_5)_3$ and intramolecular ethylene-bridged phosphine/borane also exhibited their capability for H_2 activation at room temperature (Scheme 1b and c).[18,19] In 2007, the combination of *t*-Bu_3P and $B(C_6F_5)_3$ was also shown to be capable of reacting with olefins to form zwitterionic 1,2-addition products (Scheme 1d) at room temperature.[1] Afterwards, many different types of FLP catalysts have been developed for the hydrogenation of unsaturated compounds (*e.g.* olefins, alkynes, imines, esters, ketones, aziridines, nitriles, aromatic substrates), the stoichiometric and catalytic reduction of CO_2 and the capture of environmentally harmful molecules (*e.g.* CO, CO_2, N_2O, NO, SO_2, RNSO).[2–16] Furthermore, FLP-mediated chemistry is also extended to applications in advanced organic synthesis (*e.g.* hydroamination, hydroboration, cyclization, boration, asymmetric synthesis), radical chemistry, enzyme chemistry and polymerization. Meanwhile, many new

[a] *Center for Applied Chemical Research, Frontier Institute of Science and Technology, and Shaanxi Key Laboratory of Energy Chemical Process Intensification, School of Chemical Engineering and Technology, Xi'an Jiaotong University, Xi'an 710049, China. E-mail: yongquan@mail.xjtu.edu.cn*
[b] *Department of Materials Science and Engineering City University of Hong Kong, 83 Tat Chee Avenue, Kowloon, Hong Kong, P. R. China*
[c] *Shenzhen Research Institute City University of Hong Kong Shenzhen, 518057, P. R. China*

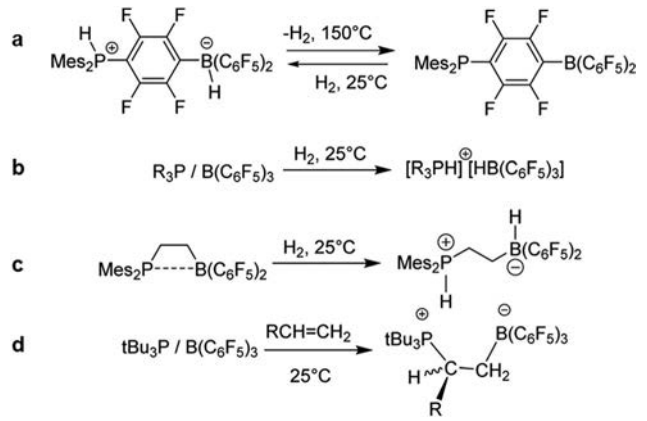

Scheme 1 Typical homogeneous FLP catalysts for hydrogen activation and the subsequent hydrogenation of olefins. Reprinted with permission from ref. 10. Copyright 2015, American Chemical Society.

types of homogeneous FLP catalysts, based on carbon, silicon and transition metals (*e.g.* Al, Zr, Ti), have also been explored for various catalytic syntheses.[2–16] We note that the concept of FLPs is not only confined to pairs that do not form Lewis acid–base adducts, but catalytic systems that provide any access to combinations of free Lewis acids and bases *via* equilibria are also considered as FLPs. Besides catalytic applications, FLP polymers constructed by integrating designer boron- or phosphorus-containing monomers as well show impressive performances as responsive self-healing gels.[20]

At present, a vast majority of chemical products are manufactured *via* heterogeneous catalytic processes. These processes often provide benefits to many different practical aspects, such as efficiently separating the reaction products from catalysts and facilitating the process scale-up for continuous production.[21] In particular, these heterogeneous catalytic processes fundamentally involve the adsorption and activation of reactants, the formation of intermediates and adsorbed products through surface reactions, and the desorption of products. This way, the surface properties of these heterogeneous catalysts would then largely determine the electronic structures of surface active sites, which significantly affect their corresponding catalytic efficiency, stability and

Yuanyuan Ma

Dr Yuanyuan Ma received her Bachelor's degree in Chemical Engineering from Nanjing University in 2002 and PhD in Chemistry from the University of California, Davis, in 2012. She is now a faculty member of the Center for Applied Chemical Research, Frontier Institute of Science and Technology, Xi'an Jiaotong University, China. Her research interests focus on heterogeneous catalysis and electrochemical catalysis by transition metals.

Sai Zhang

Dr Sai Zhang received his PhD from Xi'an Jiaotong University. He became a lecturer in the School of Chemical Engineering and Technology, Xi'an Jiaotong University, in July 2017. His research interests focus on heterogeneous catalysis in the areas of organic catalysis including selective hydrogenation, cross-coupling and dehydrogenation reactions.

Chun-Ran Chang

Dr Chun-Ran Chang received his PhD degree in Chemistry from Tsinghua University in 2013. After that he became a faculty member and now is an Associate Professor of Chemical Engineering and Technology at Xi'an Jiaotong University. His research interests focus on theoretical design of heterogeneous catalysts that are related to energy conversion, solid FLP catalysts involving the activation of small inert molecules, and catalytic mechanisms under reaction conditions. More details can be found at http://gr.xjtu.edu.cn/web/changcr/home.

Zheng-Qing Huang

Zheng-Qing Huang received his BS degree in Chemical Engineering from Xi'an Jiaotong University, China, in 2014. He is now a PhD candidate at Xi'an Jiaotong University under the supervision of Associate Professor Chun-Ran Chang. His research focuses on theoretical design of solid frustrated Lewis pair (FLP) catalysts for the activation and conversion of small inert molecules, and surface reaction mechanisms using first-principles calculations.

chemoselectivity.[21–23] In this case, when heterogeneous catalysts have tailorable physical and chemical properties on their surfaces, FLP active sites might be effectively constructed there, being analogous to that of the homogeneous counterparts. For example, the combinations of Au nanoparticles and excessive imines or nitriles were employed for the first semi-solid heterogeneous catalysts and utilized for the hydrogenation of nitriles under mild conditions.[24] A FLP-like configuration anchored on silica could also be identified by solid-state nuclear magnetic resonance (NMR).[25,26] Similarly, Ozin *et al.* reported the successful construction of a spatially separated surface Lewis base (InOH) and Lewis acid (In) pair on the surface of $In_2O_{3-x}(OH)_y$ by regulating the surface defects of oxygen vacancies, which are comparable to those of homogeneous FLPs.[27–33] Later, several semi-solid and solid FLP catalysts have been proposed, demonstrated experimentally and/or theoretically, including CeO_2,[34,35] chemical-doped two-dimensional materials,[36–38] metal organic frameworks (MOFs),[39,40] Au-Pt/WO_x,[41] Pt_x-loaded zeolite NaY,[42] $B(C_6F_5)_3$-molecular sieves,[43] polymers,[44] *etc.*

The recent advances in homogeneous FLP catalysts have been well summarized in previous reviews.[2–16] In contrast, despite great efforts on the original research of semi-solid and solid heterogeneous FLP catalysts, there has not been any comprehensive summary on this important and emerging topic. Herein, we would review the progress in constructing surface/interface FLP configurations as well as their catalytic mechanisms and applications. Our primary goal is to provide fundamental understanding of the structure–activity relationships of heterogeneous FLP catalysts. After discussing the demonstration of different heterogeneous FLP catalysts organized by the catalytic materials, challenges and future perspectives on the design and surface/interface characterization of solid FLP catalysts as well as their potential catalytic applications are included. This review aims to provide a useful resource for both academics and readers to access this topic, exploring the design and synthesis of new heterogeneous FLP catalysts along with encouraging novel technologies for the characterization of surface FLP active sites.

Brief introduction of heterogeneous FLP catalysts

In principle, heterogeneous FLP catalysts can be classified into four main types: (1) combination of a solid Lewis acid and a molecular Lewis base (Scheme 2a); (2) combination of a solid Lewis base and a molecular Lewis acid (Scheme 2b); (3) combination of a solid Lewis acid and a solid Lewis base (Scheme 2c); and (4) surface engineering of the structural defects (*e.g.*, oxygen vacancies, dopants, *etc.*) of a solid (Scheme 2d). It is noted that both type 1 and 2 catalysts involve solid acids (bases) and molecular bases (acids). Since the molecular components of these heterogeneous FLP catalysts that existed in the liquid phase are required in excess to efficiently activate target molecules in an earlier study,[24] these catalysts (*i.e.* types 1 and 2) are commonly named semi-solid FLP catalysts.

Different from conventional homogeneous FLP catalysts, regulated by a wide range of ligand selection to control the interaction between Lewis acids and bases, the surface atoms of heterogeneous catalysts are firmly held within the lattice matrix. In this case, only classic Lewis acid–base adducts can be found on the surfaces of ideal crystals. Regardless of this, it is not easy to break the classic Lewis acid–base bonding in order to create a frustrated pair. Fortunately, the "rigid" framework of solids with various structural defects and interference of environments, such as small gas molecules, ions and ligands, would provide opportunities in the design and synthesis of semi-solid and solid FLP-like

Johnny C. Ho

Dr Johnny C. Ho received his BS degree with high honors in Chemical Engineering, and MS and PhD degrees in Materials Science and Engineering from the University of California, Berkeley, in 2002, 2005 and 2009, respectively. From 2009 to 2010, he worked as a post-doctoral research fellow at Lawrence Livermore National Laboratory, California. Currently, he is an Associate Professor of Materials Science and Engineering in the City University of Hong Kong. His research interests focus on the synthesis, characterization, integration and device applications of nanoscale materials for various technological applications, including nanoelectronics, sensors and energy harvesting. Details can be found at http://www.phy.cityu.edu.hk/personal-website/johnny/site_flash/index.html.

Yongquan Qu

Dr Yongquan Qu received his BS in Materials Science and Engineering from Nanjing University in 2001, MS in Chemistry from the Dalian Institute of Chemical Physics in 2004, and PhD in Chemistry from the University of California, Davis, in 2009. He worked as a post-doctoral research fellow in the University of California, Los Angeles, from 2009 to 2011. He became a faculty member of the Center for Applied Chemical Research, Frontier Institute of Science and Technology, Xi'an Jiaotong University, China, in 2012. His research interests focus on heterogeneous catalysis in the areas of organic synthesis, clean energy production and environmental remediation. Details can be found at: http://gr.xjtu.edu.cn/web/yongquan.

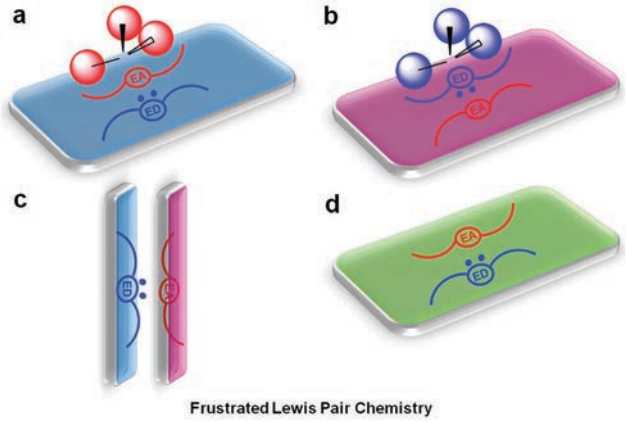

Scheme 2 Schematic chemistry of semi-solid and solid FLPs: (a) semi-solid FLP catalyst with the combination of a molecular Lewis acid and a solid Lewis base; (b) semi-solid FLP catalyst with the combination of a molecular Lewis base and a solid Lewis acid; (c) all solid FLP catalyst based on a solid Lewis acid and a solid Lewis base; and (d) all solid FLP catalyst within one solid.

catalysts. Combining the structural features of homogeneous FLPs[1–4] and the early accomplishments of heterogeneous FLP catalysts,[25–44] it can be reasonably claimed that precise controllability on their surface physicochemical properties and interfacial events are prerequisites for the construction of FLP-like heterogeneous catalysts. For semi-solid FLP catalysts, manipulation of the surface acidity or basicity of solids and proper selection of their molecular counterparts can minimize their direct surface/interface adductions to produce conventional Lewis acid–base complexes. They also preserve the appropriate distance between the solid and molecules in order to enable the accessibility of the third molecule and the subsequent activation. In the case of solid FLP catalysts, the construction of surface/interface FLP-like active sites is more complicated. For instance, chemical doping and defect modulations have been successfully developed to produce FLP catalysts of type 4.[27–38] The surface properties, including the defect population, electronic structures and spatial distribution of the surface/interface Lewis acids and Lewis bases, are critical to achieve surface/interface FLP-like active sites there. On the other hand, understanding of solid FLP catalysts of type 3 is especially sparse.[41,42] In the next section, typical semi-solid and solid FLP catalysts and their catalytic performance will be presented in detail.

Surface-modified Au nanostructures as semi-solid FLP catalysts

Despite the inert nature of bulk Au, Au nanomaterials have been extensively demonstrated to be high-performance catalysts for many chemical reactions due to their unique physicochemical properties.[45] When the size of Au catalysts is reduced to less than 2 nm, they exhibit a remarkable capability for hydrogen dissociation and subsequent hydrogenation.[45] Recently, theoretical calculations and experimental results revealed that Au nanoparticles, with a size of 50 nm, modified with imines and nitriles can also effectively activate hydrogen molecules and even hydrogenate small imines and nitriles under mild conditions.[24] These impressive catalytic behaviours originate from the constructed semi-solid FLP catalysts, where Au serves as a Lewis acid and imines/nitriles are Lewis bases. Density functional theory (DFT) calculations suggested that the weak interaction between Au particles and imines/nitriles facilitated the insertion of hydrogen molecules between them, being extremely similar to that of homogeneous FLPs. The relatively weak adsorption of imines/nitriles on the surfaces of the Au particles can also be attributed to the repulsion between the N lone pairs of the imines/nitriles and the d-band electrons of the Au surface.

Using NH_3 as a probe Lewis base, Fig. 1 illustrates the favorable orbital interaction among the Au(111) surface, H_2 and NH_3. The N lone pair and the fully filled Au d_{Z^2} would donate electrons to the σ*-antibonding orbital of H_2, suggesting the Lewis basic nature of NH_3. The partially filled Au s- and p-bands would then deplete electrons from the σ-bonding orbital of H_2. In this case, the overall net charge of the Au surface becomes negative, indicating its Lewis acidic feature. As a result, these interactions weaken the H–H bond for hydrogenation. Such systems can also be employed to hydrogenate *N*-benzylidenemethylamine and benzonitrile into the corresponding amines effectively (Scheme 3).

As compared with other heterogeneous hydrogenation catalysts, the catalytic activity of Au–H_2–imines/nitriles was found to be quite poor, revealing relatively low TOF values of 0.0021–0.0067 s^{-1}. Rossi *et al.* reported the formation of semi-solid FLP active sites on the surfaces of Au nanoparticles in the presence of N-containing bases.[46] These catalysts exhibited much higher

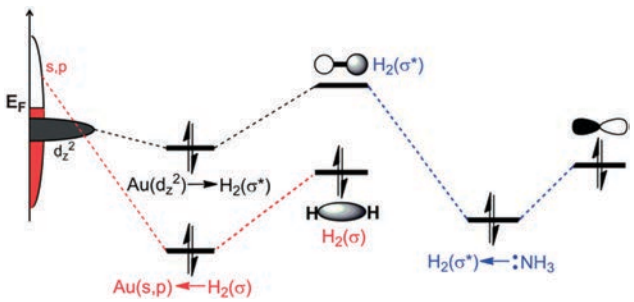

Fig. 1 Illustration of the orbital interactions of Au–H_2–NH_3. NH_3 is used as the probe molecule of imines/nitriles. Reprinted with permission from ref. 24. Copyright 2014, the Royal Society of Chemistry.

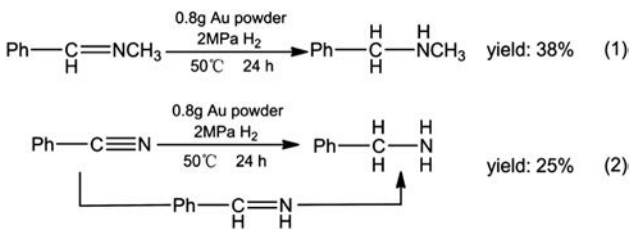

Scheme 3 Catalytic activity of the Au–H_2–imine/nitrile FLP catalysts for the hydrogenation of *N*-benzylidenemethylamine and benzonitrile. Reprinted with permission from ref. 24. Copyright 2014, the Royal Society of Chemistry.

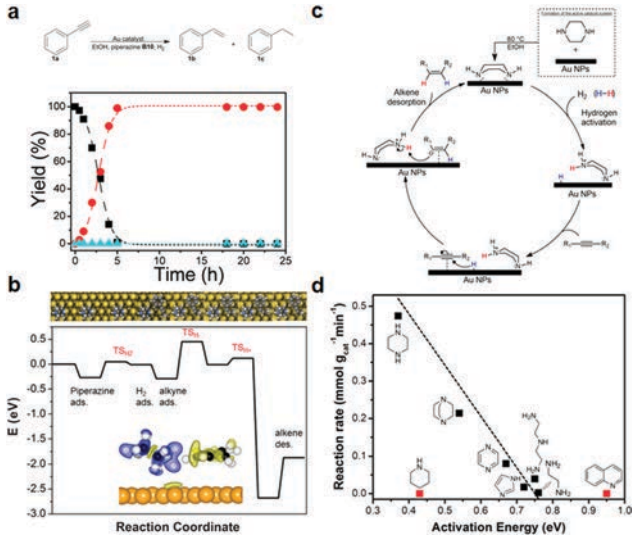

Fig. 2 Catalytic activity and mechanism of Au/N-containing base FLP catalysts. (a) Time course of the hydrogenation of phenylacetylene. Reaction conditions: 4 mmol of phenylacetylene, 0.04 mmol of Au, 4 mmol of piperazine, 8 mL of ethanol, 80 °C, 6 bar H_2. (b) Reaction energy profiles with the corresponding configurations for the hydrogenation of 1-phenyl-1-propyne. Yellow spheres represent Au, blue N, black C, and white H. (c) Proposed mechanism for the gold-catalyzed catalytic hydrogenation of alkynes into *cis*-alkenes *via* a frustrated Lewis pair approach. (d) Reaction rates (experimental) as a function of the computed activation energies for heterolytic H_2 dissociation at the Au(111)/N-containing base interface (without zero-point correction). The fitting shows that the activity is completely dominated by the H_2 activation. The red points indicate the molecules containing ligands with single N donors. Reprinted with permission from ref. 46. Copyright 2017, American Chemical Society.

activity and selectivity for the hydrogenation of alkynes into *cis*-alkenes. A wide range of N-containing bases were then examined for the hydrogenation of phenylacetylene. It was found that piperazine showed the best catalytic efficiency and nearly 100% selectivity to *cis*-alkenes. When piperazine was used as the base and the Au:phenylacetylene:base molar ratio was controlled to be 1 : 100 : 100, the completely selective hydrogenation was realized within 5 hours in ethanol at 80 °C and 0.6 MPa H_2 (Fig. 2a).

At the same time, DFT calculations show a low adsorption energy of piperazine (−0.27 eV) on the clean surface of Au. Similar to the Au–H_2–imine/nitrile system, such a weak adsorption of piperazine on the Au surface would result in the formation of a biphasic semi-solid FLP configuration, enabling the accessibility of hydrogen molecules between piperazine and the Au surface. As depicted in Fig. 2b, the hydrogen dissociation on the piperazine–Au interface requires a barrier of 0.32 eV, which is much lower than that (1.45 eV) on the Au(111) surface.[46] After the co-adsorption of alkynes, the hydride on the Au surface would overcome an energy barrier of 0.74 eV for the first step of hydrogenation. Subsequently, the proton transfer from piperazine to the intermediate would yield the selective hydrogenation with a barrier of 0.13 eV. The proposed reaction pathway is also thoroughlyillustrated in Fig. 2c.

In addition, the basicity of N-containing bases is also critical to construct interface FLP active sites. Too strong or too weak binding of these bases with the Au would contribute to their decreased hydrogenation activity or even complete loss of their catalytic capabilities. Fig. 2d displays the calculated activation energies for hydrogen dissociation at the interfaces between various N-containing bases and Au(111). It is clear that the piperazine–Au interface gives the lowest energy barrier and the fastest hydrogenation rates.

Besides the above semi-solid Au-based FLP catalysts, the highly dispersed Au on Pt/WO_x has also been reported to show an enhanced ability for H_2 activation and high catalytic performance for the selective hydrogenolysis of glycerol into 1,3-propanediol as compared with Pt/WO_x catalysts. The structural characterization studies and titration experiments suggested that these highly dispersed Au species were usually trapped at the surface defective sites and vacancies of Pt/WO_x, in particular adjacent to the surface Pt species. Such configurations are known to decrease the number of surface Lewis acidic sites and to increase the *in situ* generated Bronsted acidic sites with the assistance of H_2 through the formation of FLPs.[41]

Polymers

On the other hand, polymers are one of the most important technological materials, whose structural and electrical properties can be widely tailored, attracting significant attention for numerous applications. Among many different types of polymers, a great number of Lewis basic polymers have been rationally designed and synthesized for CO_2 capture and conversion.[47] In this case, the spatial integration of a Lewis acid and a Lewis base with the appropriate steric hindrance in a polymer may also provide another feasible approach to construct semi-solid or solid FLP catalysts. Recently, triphenylphosphine motifs as the Lewis basic sites were sterically encumbered in porous polymer networks (P1 and P2, Fig. 3a).[44] This way, adding the Lewis acid of

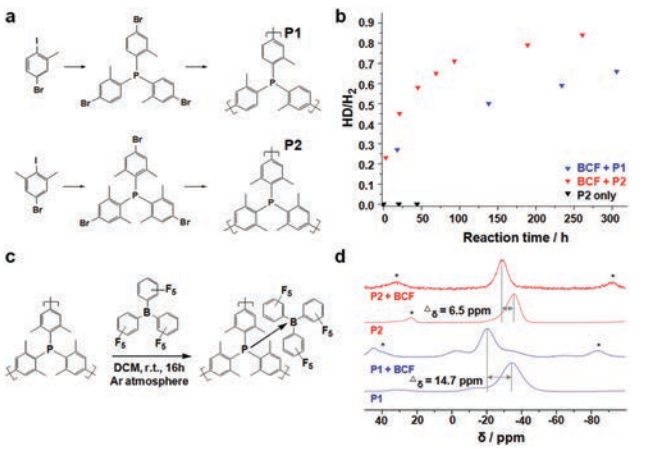

Fig. 3 Construction of semi-solid FLP catalysts between the Lewis basic porous polymer and the strong Lewis acid of $B(C_6F_5)_3$ molecules. (a) The structures of the selected triarylphosphine polymers. (b) H_2/D_2 isotope experiments for hydrogen dissociation: the plots of the integral ratios of HD/H_2 as a function of time for various catalysts. The ratios were derived from ^{1}H NMR. (c) Formation of the polymer/$B(C_6F_5)_3$ FLP catalysts and (d) ^{31}P NMR characterization. Reprinted with permission from ref. 44. Copyright 2017, American Chemical Society.

$B(C_6F_5)_3$ molecules with a large steric hindrance would lead to the formation of Lewis acid–base combinations through the interaction between P and B centers (Fig. 3b). Evidently, solid-state magic-angle spinning NMR spectroscopy of the dried combinations revealed their structural features in detail. For example, the coordination of the Lewis basic sites of these two polymers with the Lewis acid contributed to the observed downfield shift of ^{31}P signals in NMR (Fig. 3d).

Importantly, the extent of this shift was strongly dependent on the steric hindrance of triphenylphosphine derivatives. The larger hindrance around the central P atom would render a smaller shift, which suggests weaker bonding between the polymer and Lewis acid. Thus, the interaction between the polymer and Lewis acid can be modulated, facilitating the construction of semi-solid FLP catalysts. H_2/D_2 isotope experiments were also performed to demonstrate the capability and reactivity of various combinations for H_2 activation under low H_2 pressure. In particular, the polymer or solvent alone did not induce any isotope exchange, indicating that they were inactive for the heterolytic cleavage of hydrogen (Fig. 3c). In contrast, the combinations of P1/$B(C_6F_5)_3$ and P2/$B(C_6F_5)_3$ gave significant HD/H_2 ratios, revealing their capability for hydrogen dissociation and subsequent isotope exchange. In addition, P2/$B(C_6F_5)_3$ exhibited higher capability for hydrogen activation due to its larger HD/H_2 ratio as compared with that of P1/$B(C_6F_5)_3$.

Molecular sieves and zeolites

Combinations of the strong Lewis acid of $B(C_6F_5)_3$ and the Lewis base of molecular sieves (MS) or α-cyclodextrin (CD) would represent another novel class of semi-solid FLP catalysts.[43] In this configuration, the interface FLP sites can heterolytically dissociate hydrogen by the Lewis acid of $B(C_6F_5)_3$ and the Lewis base of oxygen atoms on the surface of MS or α-CD. These catalysts were found to show high catalytic activity for the hydrogenation of ketones or aldehydes into alcohols (Scheme 4a) or the reductive deoxygenation of aryl alkyl ketones and diaryl ketones into alkenes and alkanes, respectively (Scheme 4b and c).

In detail, the proposed catalytic mechanism is shown in Scheme 4d. After the hydrogen dissociation, the protonated surface oxygen of MS or α-CD binds to the oxygen atom of ketones through a hydrogen bond. The configuration of such a surface adsorbed ketone would then induce nucleophilic attack by hydride from the $HB(C_6F_5)_3$ anion. Accompanied by the recovery of FLP catalysts, the alcohol is liberated when the generated alkoxide anion receives a proton. The hydrogen bond between the ketone and alcohol can promote the C–O bond cleavage. The loss of water gives the reductive deoxygenated products of either alkenes or alkanes. Importantly, the chemoselectivity towards alcohol or deoxygenated products can be determined by the reaction conditions, Lewis base used and substrates employed (Scheme 4). The reductive oxygenation can also be catalyzed by MS/$B(C_6F_5)_3$ catalysts since the MS can absorb the generated water. Here, the MS or α-CD serves as the Lewis base to construct surface active FLP sites, facilitating the hydrogen activation and formation of hydrogen bonds. It is also

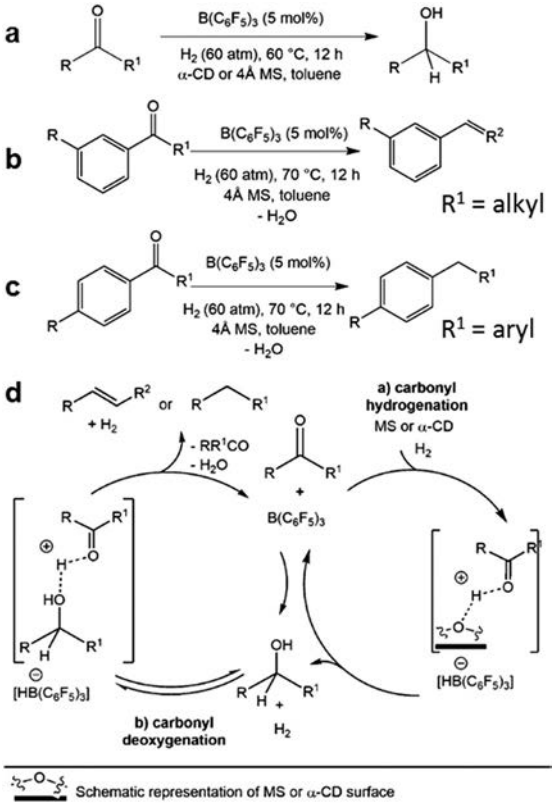

Scheme 4 Catalytic performance and mechanism of the molecular sieves/$B(C_6F_5)_3$ semi-solid FLP catalysts. (a) Hydrogenation of ketones and aldehydes. (b) Reductive deoxygenation of aryl alkyl ketones. (c) Reductive deoxygenation of diaryl ketones. (d) Proposed catalytic mechanism for the hydrogenation and reductive deoxygenation. Reprinted with permission from ref. 43. Copyright 2015, Wiley.

noted that both MS and α-CD are recyclable; however, the Lewis acids still require the renewal of $B(C_6F_5)_3$.

Furthermore, FLP active centers can also be constructed on zeolite NaY loaded with Pt nanoparticles.[42] Explicitly, Pt nanoparticles were deposited on the external surface of NaY using a Pt sputter. As shown in Fig. 4, Pt/NaY acts as the hydrogen storehouse, while Na^+ ions and framework oxygen atoms serve as the acceptors of the heterolytically cleaved hydrogen species. Initially, the hydrogen molecules are cleaved into hydrogen ions (H^+ and H^-) on the surfaces of the Pt nanoparticles. Then, the hydrides are coupled with Na^+ ions (Lewis acid), while the protons are transferred to the framework oxygen atoms (Lewis base), leading to the formation of FLP-like sites composed of Na^+H^- and framework-bound hydroxyl proton $O(H^+)$ species. The successful formation of these FLP-like catalysts was further confirmed by *in situ* neutron diffraction,[42] Na NMR spectroscopy, FTIR spectroscopy and X-ray photoelectron spectroscopy (XPS).

2D materials

In addition, many 2D materials also show promising applications in heterogeneous catalysis due to their tailorable surface properties, including their exceptionally large surface area and rich surface

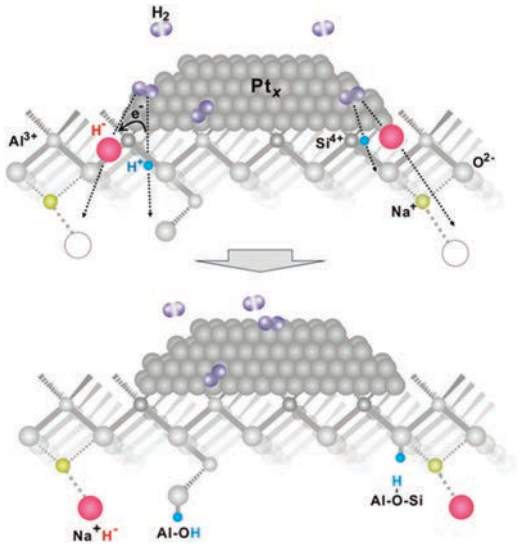

Fig. 4 Schematic illustration of the heterolytic dissociation of hydrogen on the Pt_x/NaY surface and the subsequent formation of FLP-like active sites. Reprinted with permission from ref. 42. Copyright 2015, Wiley.

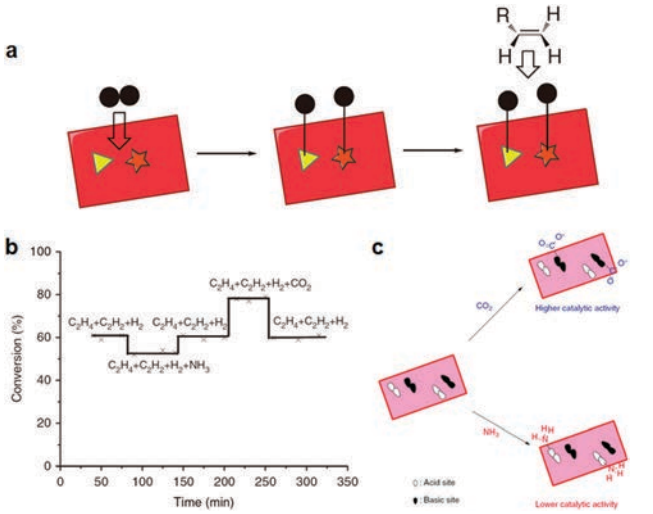

Fig. 5 (a) Proposed catalytic mechanism of graphene for hydrogenation. Triangles and stars represent the Lewis acidic and basic sites, respectively. (b) Influence of acidic or basic gases on the catalytic hydrogenation of acetylene at 100 °C. (c) Proposed FLP-like catalytic mechanism of graphene in the presence of NH_3 and CO_2. Reprinted with permission from ref. 36. Copyright 2014, Macmillan Publishers Limited.

chemistry.[48] Surface regulations on these 2D materials can then enable the construction of unique configurations of Lewis acidic sites and Lewis basic sites, which is similar to that of homogeneous FLP-like active sites. For example, introducing dopants (*i.e.* chemical doping) into the rigid lattice of 2D materials is known to produce Lewis acidic and basic sites owing to the difference in the electronegativities of the foreign and host elements. In this case, those sites with spatial controllability can be utilized to generate FLP-like active centers.

Among various 2D materials, graphene and graphene oxides have attracted great attention for their metal-free heterogeneous catalysis. Recently, graphene exhibited superior catalytic capability for the selective gas-phase hydrogenation of acetylene into ethylene and the liquid-phase hydrogenation of alkenes in the absence of any transition metals.[36] Although the exact catalytic sites of graphene for the hydrogenation had not been identified, the FLP-like catalytic mechanism could also be proposed as shown in Fig. 5a. The Lewis acid and base pairs confined in the 2D graphene at an adequate distance is believed to promote the hydrogen activation, forming surface hydric (H^-) and protic (H^+) species. Hydrogen-temperature-programmed reduction (H_2-TPR) confirmed the uptake of hydrogen by graphene, suggesting the strong interaction between hydrogen and graphene. The presence of HD in the isotope experiments as well revealed the capability of graphene for the hydrogen dissociation. Also, the titration of graphene with NH_3 and CO_2 verified the co-existence of Lewis acidic and basic sites, respectively. All the control experiments further indicate the reasonable proposal of the above-mentioned FLP-like catalytic mechanism.

In order to confirm the catalytic mechanism, the hydrogenation of acetylene was performed in a stream containing NH_3 or CO_2. As depicted in Fig. 5b, the acetylene conversion decreased by 9% in the presence of NH_3 and increased by 33% in the presence of CO_2. When the NH_3 or CO_2 gas was switched off, the catalytic performance of graphene was almost restored to the initial state. It was considered that NH_3 blocked the Lewis acidic sites of graphene under the reaction conditions, leading to decreased catalytic activity. Meanwhile, CO_2 formed a carboxylate-like group in graphene and subsequently promoted the hydrogen activation with the surface Lewis basic sites. However, it is quite surprising that the catalytic activity of graphene was not completely quenched in the presence of NH_3. Moreover, although the introduction of foreign atoms into graphene can generate more Lewis acidic/basic sites, the presence of heteroatoms (*e.g.* N, P, S) within the graphene lattice was found to decrease both the catalytic activity and selectivity with an increasing amount of dimerized/oligomerized compounds as the by-products. All these catalytic phenomena would suggest that further structural characterization and mechanistic studies on the hydrogenation activity of graphene are necessary.

At the same time, theoretical calculations predict that it is also possible to construct FLP-like active sites for the hydrogen activation in the boron and nitrogen co-doped bilayer graphene (BN-G) and graphene ribbon (BN-GR).[38] This configuration uniquely features the nitrogen and boron atoms separated in different layers with a suitable distance, which can overcome an energy barrier of 0.43 eV for the heterolytic cleavage of hydrogen molecules. Meanwhile, it inevitably raises the challenge to the synthesis of such catalysts featuring delicate bilayer graphene structures along with spatially controllable B/N codopants.

Similarly, B- or Al-doped 2D phosphorenes were also theoretically predicted to form FLPs effectively without the need for any steric hindrance there.[37] Two possible pathways for the corresponding hydrogen activation were then proposed. In the first one, the hydrogen molecule is split and the activated hydrogen species react subsequently with the adsorbed unsaturated molecules. Alternatively, the hydrogen molecule directly hydrogenates the

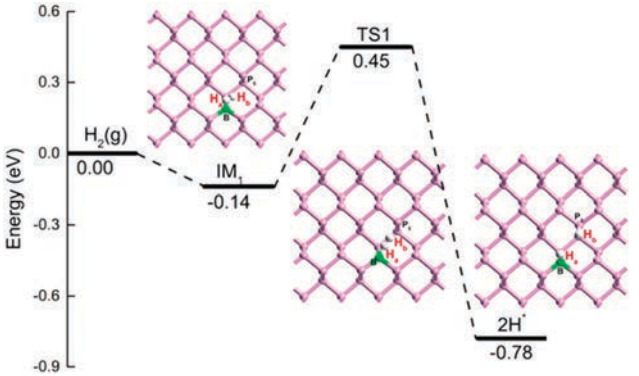

Fig. 6 Energy profile of the hydrogen activation on the surfaces of B-doped phosphorenes. Reprinted with permission from ref. 37. Copyright 2017, American Chemical Society.

adsorbed molecule. Fig. 6 shows the energy profile of hydrogen activation on the B-doped phosphorenes. The physically adsorbed hydrogen has to overcome an energy barrier of 0.59 eV for the surface hydrogen dissociation. The heterolytic cleavage then forms the hydridic and protic hydrogen on B (Lewis acid) and P (Lewis base), respectively. Further calculations indicate that the hydrogen diffusion along B-doped phosphorenes is endothermic, which requires a very large energy barrier. Therefore, such configurations and catalytic behaviors are observed to be very similar to those of homogeneous FLPs. In contrast, the second pathway has to come across much higher reaction barriers as compared with those through the first pathway. The calculations also suggest that the electron-deficient Al can serve as the dopant, further decreasing the energy barrier for hydrogen activation on the surfaces of the Al-doped phosphorenes.

CeO_2

Apart from 2D nanomaterials, transition metal oxide nanostructures, especially CeO_2 nanostructures, also exhibit promising applications as supports, additives and active components for heterogeneous catalysis due to their reversible Ce^{3+}/Ce^{4+} redox pairs under mild conditions. The surface defects induced by the reducible/oxidizable valence states of cerium are typically accompanied by the newly constructed surface Lewis acidic sites and Lewis basic sites on the surface of CeO_2. At the same time, the rigid lattice of solids provides similar steric hindrance, which is commonly observed in homogeneous FLP catalysts.[34] Thus, it is possible to construct surface FLP-like active sites when the surface oxygen atom functions as the Lewis base, existing in a close proximity to the surface defects as the Lewis acid. Based on DFT calculations on the $CeO_2(110)$ surface, it is likely to create novel surface Lewis acidic sites when two adjacent lattice oxygen atoms are removed (Fig. 7a). In this configuration, the reduced Ce cations (Ce_I and Ce_{II}) and surface lattice oxygen (O_{IIc}) are the independent Lewis acid and base, respectively. Thus, the Ce_I–O_{Ic} and Ce_{II}–O_{IIc} species may serve as surface FLP-like active sites, being similar to those of molecular FLPs. As compared with the Ce_I–O_{IIc} and Ce_{II}–O_{IIc} configurations, the distance between the Lewis acidic site and Lewis basic site of the FLP configuration is 3.99 Å (Fig. 7a), which is comparable to those of homogenous FLP catalysts for hydrogen activation. Moreover, stronger charge contraction by these two adjacent Ce^{3+} Lewis acids is anticipated to show higher capability for the hydrogen activation. DFT calculations as well reveal the possibility to construct similar FLP active sites on the CeO(100) surface; however, the fabrication of surface FLP sites cannot be realized by simply removing surface oxygen atoms on the $CeO_2(111)$ facet.

According to the above discussion, it is therefore challenging to form defect clusters and difficult to create active sites at a low concentration of surface defects (Fig. 7a). In contrast, it is possible to realize the construction of surface FLP catalytic sites on CeO_2 with abundant surface defects. Recently, a two-step hydrothermal method was developed to synthesize porous nanorods of CeO_2 (PN-CeO_2) with a high surface Ce^{3+} fraction

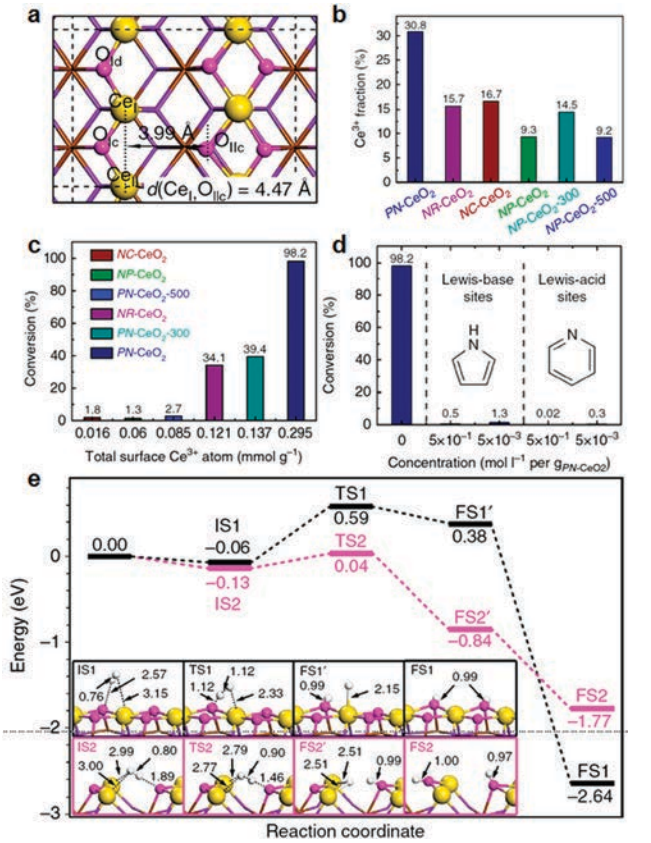

Fig. 7 Surface regulations on CeO_2 for the construction of surface FLP-like catalytic sites and their performance for hydrogenation. (a) DFT calculations on the possibility by the surface regulations for the formation of independent surface Lewis acidic sites and Lewis basic sites on $CeO_2(110)$ and the construction of surface FLP sites. (b) Surface fractions of Ce^{3+} for various CeO_2. (c) Catalytic hydrogenation activity *versus* the surface fractions of Ce^{3+}. Reaction conditions: styrene (1.0 mmol), toluene (0.5 ml) and catalysts (20.0 mg) at 100 °C and 1.0 MPa H_2 pressure for 14 h. (d) Influences of a molecular Lewis-base or Lewis-acid on the catalytic activity of PN-CeO_2 for the hydrogenation of styrene. (e) Energy profiles for H_2 dissociation on ideal $CeO_2(110)$ in the black curve and $CeO_2(110)$ with two oxygen vacancies in the red curve. The optimized structures of the initial states (IS), transition states (TS) and final states (FS) are labelled with bond distances (in Å). Reprinted with permission from ref. 34. Copyright 2014, Macmillan Publishers Limited.

and a large concentration of oxygen vacancies. As predicted, PN-CeO_2 displayed high catalytic activity for the hydrogenation of alkynes and alkenes. The surface Ce^{3+} fraction can also be used as a descriptor to characterize the surface defects. As shown in Fig. 7b and c, the decrease of the surface Ce^{3+} fraction was found to significantly reduce the catalytic activity for the hydrogenation of styrene. All control experiments evidently suggest that the coexistence of surface Lewis acidic and basic sites plays extremely important roles in activating hydrogen molecules under mild catalytic conditions and achieving high catalytic activity for subsequent hydrogenation. In order to confirm the formation of FLP-like catalytic centers there, the analogous aspects between molecular FLP catalysts and PN-CeO_2 are listed as follows: (1) the independent surface Lewis acidic and basic sites of PN-CeO_2 (Fig. 7a); (2) the close proximity ($\sim$4 Å) between the surface Lewis acidic and basic sites for the activation or splitting of small molecules; and (3) the completely quenched hydrogenation activity with the addition of other molecular Lewis acids or bases (Fig. 7d).

The high activity of such CeO_2-based solid FLP sites towards the activation of small molecules can be further validated with the study of the dissociative activation of H_2 on the ideal CeO_2(110) and reduced CeO_2(110) surfaces. The calculated energy barrier for the heterolytic splitting of hydrogen was determined to be only 0.17 eV, being much lower than that (0.65 eV) on the ideal CeO_2 surface (Fig. 7e). Very recently, our DFT calculations also show that the creation of surface oxygen vacancies can enhance both the acidity of FLP-acid sites (Ce ions) and the basicity of FLP-base sites (O ions).[35] The enhanced acidity and basicity together with the elongated distance between FLP sites can contribute to the enhanced activity of solid FLPs for the hydrogen dissociation. This way, the heterolytic cleavage of H_2 is accelerated at FLP sites with a decrease of the activation barrier of 0.48 eV on CeO_2(110) and 0.30 eV on CeO_2(100) surfaces. By analyzing the geometric and electronic structures of adsorbed H_2 along the dissociation reaction, it has been found that relatively early transition states can be achieved on FLPs. The interaction between H_2 and FLP sites can also yield a lower energy-level $H_2\cdots$FLP bonding state. Furthermore, in contrast to the phenomenon commonly observed in stoichiometric CeO_2 that the dissociated hydride ($H^{\delta-}$) adsorbed on Ce sites is prone to transfer to the more stable O sites, the $H^{\delta-}$ on FLPs can be stabilized at Ce sites, forming a dihydrogen bond with the dissociation proton ($H^{\delta+}$) there. As shown in Fig. 8, the hydrogenation of acetylene at FLP sites can be initiated by attacking the hydrides adsorbed on Ce sites by avoiding the formation of C–O bonds, which results in relatively low activation energies of the rate-determining step at solid FLPs with 0.58 eV on CeO_2(110) and 0.88 eV on CeO_2(100) surfaces. These results would provide important insights into the mechanism of H_2 activation and acetylene hydrogenation at FLPs on the metal oxide surface.

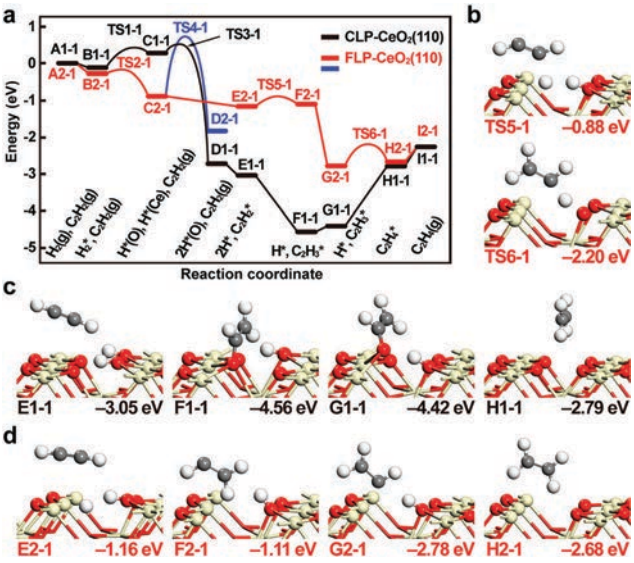

Fig. 8 Partial acetylene hydrogenation on CeO_2(110). (a) Potential energy diagram of the reactions on CLP sites (the black curve) and FLP sites (the red and blue curves). (b–d) Selected geometric structures of the transition states and intermediates. Reprinted with permission from ref. 35. Copyright 2018, American Chemical Society.

$In_2O_{3-x}(OH)_y$

Similarly, Ozin *et al.* reported the FLP-like catalytic behavior of $In_2O_{3-x}(OH)_y$ nanocrystals for the activation of CO_2 and H_2, where the surfaces of the metal oxides contained interfacial independent Lewis acidic sites (In) and Lewis basic sites (InOH).[27–33] The co-existence of oxygen vacancies and interface OH species is critical to create the required surface for these FLP-like active centers. A typical FLP-like structure of InOH/In is presented in Fig. 9a.[28] In particular, the $In_2O_{3-x}(OH)_y$ catalysts

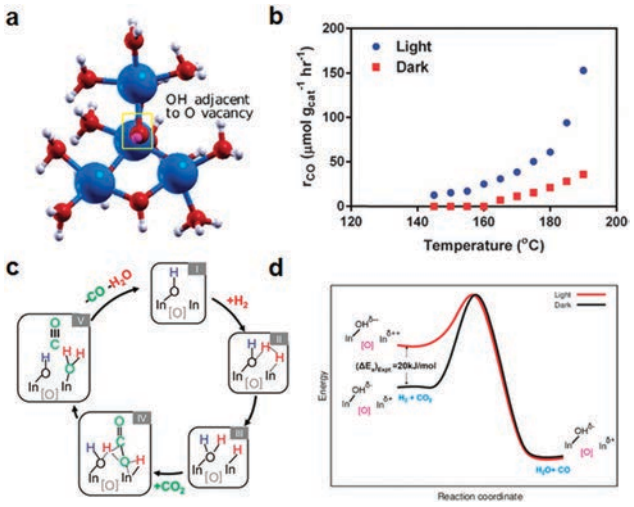

Fig. 9 FLP-like catalytic performance of the $In_2O_{3-x}(OH)_y$ catalysts for the selective hydrogenation of CO_2 into CO. (a) Geometric structure of $In_2O_{3-x}(OH)_y$ with an FLP analogy composed of an unsaturated In species as the Lewis acid, an In–OH species as the Lewis base and an oxygen vacancy. (b) Catalytic performance of $In_2O_{3-x}(OH)_y$ in the dark or under light irradiation. (c) Proposed catalytic mechanism. (d) Illustration of the origin of the difference in the activation energy for the selective hydrogenation of CO_2 in the dark and under light irradiation. (a and d) Reprinted with permission from ref. 28. Copyright 2016, American Chemical Society. (b and c) Reprinted with permission from ref. 27. Copyright 2015, Royal Chemical Society.

exhibit both thermochemical and photochemical activities for the selective conversion of CO_2 into CO with H_2 as the reducing agent (Fig. 9b).[27] It was noted that the thermo-reduction of CO_2 could be initiated at 165 °C in the dark. In contrast, a CO production rate of 15.4 μmol g_{cat}^{-1} h^{-1} was observed at 140 °C under light irradiation with identical gas flow rates of CO_2 and H_2. The calculated apparent activation energy of the photo-reduction process was ~86 kJ mol^{-1}, which was smaller than that of the thermoreduction process (107 kJ mol^{-1}). Through the complementary experiments and DFT calculations, the catalytic mechanism is proposed in detail in Fig. 9c.[27] In the first step, the adsorbed H_2 molecule on the catalytic sites undergoes heterolytic cleavage, forming the hydridic In–H^- and protonic In–OH_2^+ species. The CO_2 molecule is then adsorbed at the surface site composed of an oxygen vacancy, a hydridic In–H^- and a protonic In–OH_2^+, where the site can selectively dissociate CO_2 into CO along with the formation of H_2O. Afterwards, the desorption of CO and H_2O will re-generate the surface FLP-like active centers. Recent metadynamics-based *ab initio* molecular dynamics studies have suggested that the reduction of CO_2 is the rate determining step. The enhanced catalytic activity of the $In_2O_{3-x}(OH)_y$ catalysts can be attributed to the formation of the more acidic surface of unsaturated In sites and the more basic surface of In–OH under light irradiation. As a result, the more positively charged surface Lewis acid and more negatively charged surface Lewis base can be employed to promote the hydrogen dissociation and to lower the activation barrier of H_2 activation (Fig. 9d).[28] The produced H_2O molecule tends to be dissociatively adsorbed rather than molecularly desorbed, which may then block the surface FLP-like catalytic centers. Recently, the lifetime of photoexcited carriers is found to be prolonged in the superstructures composed of small $In_2O_{3-x}(OH)_y$ nanocrystals. Consistently, these assembled species exhibited a higher catalytic activity for the selective hydrogenation of CO_2 into CO under light irradiation.[29]

In any case, it is not necessarily true that every oxygen vacancy site substituted with the OH of the $In_2O_{3-x}(OH)_y$ nanocrystal can serve as the active site for the activation of small molecules.[32] Only those sites composed of InOH/In pairs are active for the activation, while other sites usually produce the classic Lewis acid–base complex. In this structure (Fig. 9a), the oxygen vacancy forms electron-rich surface sites, which results in the formation of unsaturated surface In sites as the Lewis acid adjacent to the surface Lewis base of In–OH. In order to evaluate the influence of these oxygen vacancy sites on the photocatalytic conversion of CO_2, $In_2O_{3-x}(OH)_y$ catalysts, with various controllable concentrations of oxygen vacancies, were prepared by varying the calcination temperatures during synthesis.[33] It was found that the higher concentration of oxygen vacancies could promote the photo-catalytic activity. Femtosecond transient absorption measure-ments also suggested that the higher concentration of surface defects would give longer excited-state lifetimes of the photo-generated charges for the catalysts. These longer lifetimes are critical for the charge separation between the surface Lewis acidic In sites and Lewis basic InOH species, which consequently enhance the catalytic efficiency.

Challenges and future perspectives in the design and synthesis of heterogeneous FLP catalysts

Heterogeneous FLP catalysts undoubtedly exhibit tremendous potential for the activation of small inert molecules in various advanced catalytic reactions. Summarizing from the successful cases, there are still very limited examples reported as efficient semi-solid and solid FLP catalysts, which indicates the substantial difficulties but great potential to further enhance their design and synthesis for the industrial deployment. It inevitably raises the demand for an improved synthesis of heterogeneous FLP catalysts, detailed characterization of surface FLP active sites and careful evaluation of catalytic mechanisms at molecular levels.

First of all, the synthesis of heterogeneous FLP catalysts is not straightforward due to the lack of effective methods to manipulate a solid surface to construct frustrated Lewis acid–base pair-sites at a precise level. In order to enable the rational design and successful synthesis of heterogeneous FLP catalysts, several critical aspects, including the material choice, inter-action manipulation between a Lewis acid and base, spatial architecture of the interfacial Lewis acidic and basic sites, Lewis acidity/basicity, crystallinity, *etc.*, have to be carefully considered. The Lewis acidity/basicity of solids is generally determined by their ionic strength, charge, ionic radius, coordination number and geometrical and electronic structures. Thus, it is extremely important to select the appropriate elements to design FLP catalysts with specific applications.

Manipulating the interaction between Lewis acids and bases is also essential to construct solid FLP configurations. Too strong interaction would lead to the formation of classic Lewis acid–base complex species. Conversely, too weak interaction would cause them to lose their capability for the activation of target molecules. The spatial distance between the Lewis acid and base is therefore an important parameter here. The longer distance would make it difficult for the accessibility and the subsequent activation of target molecules through the homogeneous FLP-like pathway. Such rigorous requirements for the construction of surface active FLP sites inevitably raise the difficulty in the synthesis of catalysts with a well-defined elemental and/or defect distribution. Until now, there has not been any effective approach to realize precise controllability on both the location and distribution of the dopants or structural defects at the atomic level. In most cases, the overall concentration of dopants or surface defects can be revealed macroscopically using various characterization techniques, providing information to guide the construction of FLP-like sites in semi-solids and solids. For CeO_2 and $In_2O_{3-x}(OH)_y$, the formation of FLP-like active sites is significantly dependent on the population of various oxygen vacancy defects, where the high concentration of surface defects would lead to a higher possibility to form surface FLP active sites.[27–35] In the case of FLP sites induced by chemical doping, the Lewis acidity and basicity can be modulated by the types and concentrations of the dopants. The spatial configurations of both surface Lewis acidic sites and basic sites are also governed by the

elemental dopant concentration and distribution of the solid. For semi-solid FLP catalysts, the efficacies of molecular Lewis acids (bases) and/or those of the corresponding solid Lewis bases (acids) have to be well balanced in order to realize frustrated Lewis acid–base pairs.

Besides, the size, crystallinity and morphology can as well affect the local acidity and basicity due to the different surface energies, bonding, electronic structures, *etc.*, in different environments. Solid catalysts with very small dimensions (*e.g.* nanoscale) can generate more surface sites with lower coordination numbers, which lead to the varied efficacies of surface Lewis acidic or basic sites. Also, the larger surface area-to-volume ratios of nanomaterials can provide more effective sites for the construction of surface FLP active sites and eventually produce a greater number of active sites.

Among various approaches, incorporating Lewis acidic and basic pairs into metal–organic frameworks (MOFs) might be an ideal platform to construct heterogeneous FLP catalysts. In MOF configurations, the chemical composition and structure can be well-defined, which can be effectively utilized for catalysis. Due to the rich chemistry of organic ligands, MOF configurations provides another flexible scheme to control the efficacies of Lewis acids or bases by manipulating the functionalized ligands with the desired substituent groups. Recent theoretical calculations suggest that it is also possible to construct solid FLP MOF catalysts (UiO-66 series, Fig. 10) for the hydrogenation of CO_2.[39,40] In particular, the hydrogen molecule is heterolytically dissociated in UiO-66-P-BF_2, where one hydrogen atom is bound to B, while another hydrogen atom is linked to N (Fig. 10a). The activated hydrogen species can then hydrogenate CO_2 into HCOOH through a concerted addition with an energy barrier of 0.28 eV. Their capability for the activation of hydrogen can also be effectively tuned by incorporating Lewis pairs (Fig. 10b). To date, the research progress in MOF-based FLPs has remained at the level of theoretical simulations, leaving the opportunities to their chemical synthesis as well as assessing their corresponding catalytic performances.

Second, the stability of semi-solid and solid FLP catalysts after exposure to ambient conditions or reaction environments is also a serious concern. The adsorption of foreign species on the surface Lewis acidic/basic sites of solid catalysts might be destructive to the formation of any subsequent FLP site, especially when the size of the solid catalysts reaches nanoscale. After their exposure to ambient conditions, the interfacial Lewis acidic/basic sites on the solid catalysts can become active sites for the adsorption of small environmental molecules (*e.g.* H_2O, CO_2). Thus, these small molecules can then block the surface Lewis acidic or basic sites and eventually prevent the formation of surface FLP-like configurations, particularly when the strong binding between those molecules and surface sites exists. The solvents can also get adsorbed chemically onto the surface Lewis acidic and/or basic sites. For example, the amines can donate electrons from the lone electron pair of nitrogen to the surface electron deficient sites, occupying the surface Lewis acidic sites. Too strong and irreversible adsorption would lead to the failure of the formation of FLP-like sites. Therefore, the removal or manipulation of adsorbed species without any interference of surface Lewis acidic and/or basic sites is an essential prerequisite for the construction of heterogeneous FLP catalysts. In any case, it is still uncertain for any dynamic change on the interfacial Lewis acidic and basic sites under the conditions of catalytic reactions. The effects of reaction temperatures and reactive pressures on the surface FLP-like sites are still not well understood at the moment.

Third, the characterization of surface FLP-like catalytic sites is still quite limited by the current technologies. Appropriate methods or techniques, which can provide the most incisive determination of the structural features of the interested interfacial Lewis acid–base pair-site, are essential to evaluate the catalytically active sites. All these are important to further understand their cooperative pathways with the target molecules. Although several examples of semi-solid and solid FLP catalysts have been proposed, the FLP-like performance is mainly assessed based on (1) the quenched catalytic activity upon the addition of small amounts of other small Lewis acids or Lewis bases and (2) the DFT calculations. Many methods, such as Fourier transform infrared spectroscopy (FTIR), temperature-programmed adsorption/desorption and calorimetric enthalpy of adsorption, can be employed to quantify the strength of the surface Lewis acid and Lewis base. However, there is no effective indicator or descriptor to describe the unbonded Lewis acid/base pairs on the surface/interface of semi-solid and solid catalysts. Also, there is no theory established to predict the mechanism involved and the reactivity of such a surface active site. Thus, it is extremely desired that advanced techniques be developed to probe surface FLP-like active centers, directly visualizing the catalytic sites. The obtained information would be extremely useful to understand the formation of surface FLP sites as well as to establish design guidelines for the improved FLP catalyst.

Among various techniques, solid-state NMR may be a feasible tool to identify the basicity and acidity of heterogeneous FLP catalysts by providing structural information of solid catalysts, including the concentration, strength, local chemical environments and even average distances between the Lewis acidic and basic sites.[49,50] Xing *et. al.* reported solid FLP [$\equiv$SiOB(C_6F_5)$_2$]-[*t*-Bu_3P] catalysts by the conjugation of Lewis acid BH(C_6F_5)$_2$ on

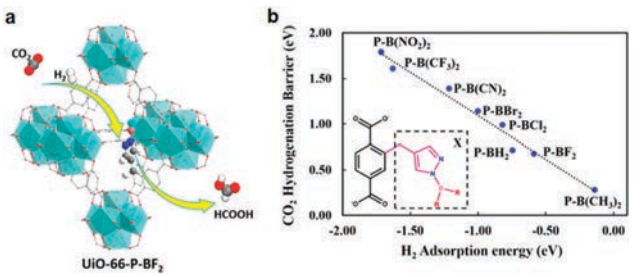

Fig. 10 (a) Structural configuration of UiO-66-P-BF_2 and illustration of the activation of H_2 and the hydrogenation of CO_2. P-BF_2 represents 1-(difluoroboranyl)-4-methyl-1*H*-pyrazole. (b) The calculated energy barriers for the hydrogenation of CO_2 as a function of H_2 adsorption energy in the UiO-66 series. Reprinted with permission from ref. 39 and 40. Copyright 2015, American Chemical Society.

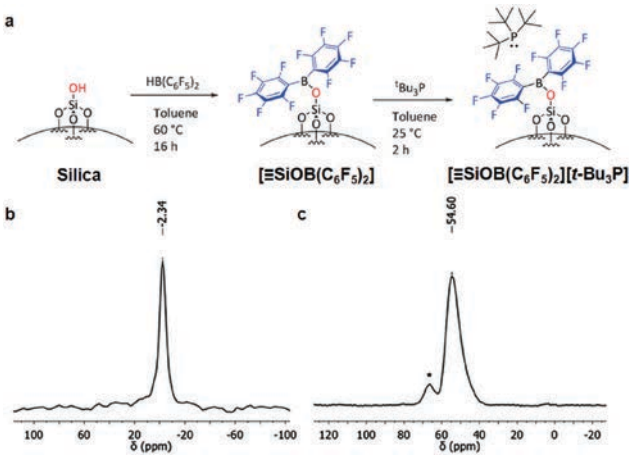

Fig. 11 (a) Schematic illustration of solid FLP catalysts: [≡SiOB(C_6F_5)$_2$]-[t-Bu_3P]. (b) Solid state ^{11}B–^{1}H CP MAS NMR spectrum of the FLP catalysts under hydrogen at a 10 kHz spinning rate. (c) Solid state ^{31}P–^{1}H CP MAS NMR spectrum of the FLP catalysts under hydrogen at a 10 kHz spinning rate. Reprinted with permission from ref. 26. Copyright 2016, Royal Chemical Society.

silica and the subsequent treatment with stoichiometric t-Bu_3P (Fig. 11a).[26]

The successful activation of hydrogen and the formation of B–H and P–H bonds could be examined using the ^{11}B–^{1}H CP MAS NMR (Fig. 11b) and ^{31}P–^{1}H CP MAS NMR (Fig. 11c) spectra, respectively.

Fourth, the atomic-level understanding of the catalytic pathway of heterogeneous FLP catalysts is still lacking. In general, DFT calculations can reveal the intermediates of reactions, predict the active species and provide insights into the catalytic mechanism. However, current DFT studies are commonly simplified to minimize calculation efforts on the designated surface of interested catalysts, which cannot fully describe the realistic reaction environments and complicated surface states of catalysts. The computational methodology should as well be improved towards the modelling of real catalytic systems. Recently, meta-dynamics based *ab initio* molecular dynamics calculations have been successfully employed to understand the FLP reaction pathways for the hydrogenation of CO_2 catalyzed by $In_2O_{3-x}(OH)_y$ catalysts;[17] nevertheless, better models closer to the practical operating conditions are still needed. Besides, various *in situ* techniques, such as XPS, FTIR, and synchrotron radiation, may also be used to collect valuable information, which will help in further understanding the catalytic pathway of heterogeneous FLP catalysts.

Fifth, the reaction scope of heterogeneous FLP catalysts is often limited. The unsaturated molecules and their derivatives usually contain functional groups with Lewis acidity and/or basicity, which might occupy the FLP active sites and then block their catalytic activities. Therefore, catalysts with extended substrates are expected to be carefully designed, developed and synthesized.

Conclusions

In summary, recent efforts in exploring heterogeneous FLP catalysts have revealed their technological potential and advantages for the activation of small inert molecules for catalysis. However, the relatively slow development of this research area also suggests the difficulty in the design and synthesis of these solid FLP catalysts. In this work, we give a foretaste of many possibilities in this emerging field. Importantly, it is essential to gain further insights by carefully evaluating the relationship between surface modulations/engineering and construction of FLP-like active sites on the solid surface, which may call for the reconsideration of conventional acidic/basic surfaces with facile and exciting catalytic phenomena. The past and present progress can also ultimately facilitate the rapid development of this brand new discipline of surface chemistry, where deep understanding would benefit the rational design and preparation of catalysts, recognize the connection between homogeneous and heterogeneous catalysis, and explore their potential applications in advanced synthetic chemistry and other utilizations.

Conflicts of interest

There are no conflicts to declare.

Acknowledgements

We acknowledge the financial support from the National Natural Science Foundation of China (Grant 21401148, 21603170 and 91645203) and the National 1000-Plan program. Prof. Y. Qu is also supported by the Cyrus Tang Foundation through the Tang Scholar program.

Notes and references

1 J. S. J. McCahill, G. C. Welch and D. W. Stephan, *Angew. Chem., Int. Ed.*, 2007, **46**, 4968–4971.
2 D. W. Stephan and G. Erker, *Angew. Chem., Int. Ed.*, 2010, **49**, 46–76.
3 D. W. Stephan, *Acc. Chem. Res.*, 2015, **48**, 306–316.
4 D. W. Stephan, *Science*, 2016, **354**, aaf7229.
5 J. Paradies, *Angew. Chem., Int. Ed.*, 2014, **53**, 3552–3557.
6 Y. B. Liu and H. F. Du, *Acta Chim. Sin.*, 2014, **72**, 771–777.
7 D. W. Stephan and G. Erker, *Chem. Sci.*, 2014, **7**, 2625–2641.
8 D. W. Stephan and G. Erker, *Angew. Chem., Int. Ed.*, 2015, **54**, 6400–6441.
9 D. W. Stephan, *J. Am. Chem. Soc.*, 2015, **137**, 10018–10032.
10 A. J. P. Cardenas, Y. Hasegawa, G. Kehr, T. H. Warren and G. Erker, *Coord. Chem. Rev.*, 2016, **306**, 468–482.
11 J. M. Bayne and D. W. Stephan, *Chem. Soc. Rev.*, 2016, **45**, 765–774.
12 G. Kehr and G. Erker, *Chem. Rec.*, 2017, **17**, 803–815.
13 S. Arndt, M. Rudolph and A. S. K. Hashmi, *Gold Bull.*, 2017, **50**, 267–282.
14 F. G. Fontaine, M. A. Courtemanche, M. A. Legare and E. Rochette, *Coord. Chem. Rev.*, 2017, **334**, 124–135.
15 D. J. Scott, M. J. Fuchter and A. E. Ashley, *Chem. Soc. Rev.*, 2017, **46**, 5689–5700.

16 W. Meng, X. Q. Feng and H. F. Du, *Acc. Chem. Res.*, 2018, **51**, 191–201.
17 G. C. Welch, R. R. S. Juan, J. D. Masuda and D. W. Stephan, *Science*, 2006, **314**, 1124–1126.
18 G. C. Welch and D. W. Stephan, *J. Am. Chem. Soc.*, 2007, **129**, 1880–1881.
19 P. Spies, G. Erker, G. Kehr, K. Bergander, R. Kröhlich, S. Grimme and D. W. Stephan, *Chem. Commun.*, 2007, 5072–5074.
20 M. Wang, F. Nudelman, R. R. Matthes and M. P. Shaver, *J. Am. Chem. Soc.*, 2017, **139**, 14232–14236.
21 R. Schlögl, *Angew. Chem., Int. Ed.*, 2015, **54**, 3465–3520.
22 J. A. Rodriguez, D. C. Grinter, Z. Liu, R. M. Palomino and S. D. Senanayake, *Chem. Soc. Rev.*, 2017, **46**, 1824–1841.
23 F. Tao and P. A. Crozier, *Chem. Rev.*, 2016, **116**, 3487–3539.
24 G. Lu, P. Zhang, D. Q. Sun, L. Wang, K. B. Zhou, Z. X. Wang and G. C. Guo, *Chem. Sci.*, 2014, **5**, 1082–1090.
25 K. C. Szeto, W. Sahyoun, N. Merle, J. L. Castelbou, N. Popoff, F. Lefebvre, J. Raynaud, C. Godard, C. Claver, L. Delevoye, R. M. Gauvin and M. Taoufik, *Catal. Sci. Technol.*, 2016, **6**, 882–889.
26 J. Y. Xing, J. C. Buffet, N. H. Rees, P. Norby and D. O'Hare, *Chem. Commun.*, 2016, **52**, 10478–10481.
27 K. K. Ghuman, T. E. Wood, L. B. Hoch, C. A. Mims, G. A. Ozin and C. V. Singh, *Phys. Chem. Chem. Phys.*, 2015, **17**, 14623–14635.
28 K. K. Ghuman, L. B. Hoch, P. Szymanski, J. Y. Y. Loh, N. P. Kherani, M. A. E-Sayed, G. A. Ozin and C. V. Singh, *J. Am. Chem. Soc.*, 2016, **138**, 1206–1214.
29 L. He, T. E. Wood, B. Wu, Y. C. Dong, L. B. Hoch, L. M. Reyes, D. Wang, C. Kubel, C. X. Qian, J. Jia, K. Liao, P. G. O'Brien, A. Sandhel, J. Y. Y. Loh, P. Szymanski, N. P. Kherani, T. C. Sum, C. A. Mims and G. A. Ozin, *ACS Nano*, 2016, **10**, 5578–5586.
30 L. B. Hoch, L. He, Q. Qiao, K. Liao, L. M. Reyes, Y. M. Zhu and G. A. Ozin, *Chem. Mater.*, 2016, **28**, 4160–4168.
31 M. Ghoussoub, S. Yadav, K. K. Ghuman, G. A. Ozin and C. V. Singh, *ACS Catal.*, 2016, **6**, 7109–7117.
32 K. K. Ghuman, L. B. Hoch, T. E. Wood, C. Mims, C. V. Singh and G. A. Ozin, *ACS Catal.*, 2016, **6**, 5764–5770.
33 L. B. Hoch, P. Szymanski, K. K. Ghuman, L. He, K. Liao, Q. Qiao, L. M. Reyes, Y. M. Zhu, M. A. E-Sayed, C. V. Singh and G. A. Ozin, *Proc. Natl. Acad. Sci. U. S. A.*, 2016, **113**, E8011–E8020.
34 S. Zhang, Z.-Q. Huang, Y. Y. Ma, W. Gao, J. Li, F. X. Cao, L. Li, C.-R. Chang and Y. Qu, *Nat. Commun.*, 2017, **8**, 15266.
35 Z.-Q. Huang, L.-P. Liu, S. Qi, S. Zhang, Y. Qu and C.-R. Chang, *ACS Catal.*, 2018, **8**, 546–554.
36 A. Primo, F. Neatu, M. Florea, V. Parvulescu and H. Garcia, *Nat. Commun.*, 2014, **5**, 5291.
37 J. X. Zhao, X. Y. Liu and Z. F. Chen, *ACS Catal.*, 2017, **7**, 766–771.
38 X. Y. Sun, B. Li, T. F. Liu, J. Song and D. S. Su, *Phys. Chem. Chem. Phys.*, 2016, **18**, 11120–11124.
39 J. Y. Ye and J. K. Johnson, *ACS Catal.*, 2015, **5**, 2921–2928.
40 J. Y. Ye and J. K. Johnson, *ACS Catal.*, 2015, **5**, 6219–6229.
41 X. C. Zhao, J. Wang, M. Yang, N. Lei, L. Li, B. L. Hou., S. Miao, X. L. Pan, A. Wang and T. Zhang, *ChemSusChem*, 2017, **10**, 819–824.
42 H. Lee, Y. N. Choi, D. W. Lim, M. M. Rahman, Y. I. Kim, I. H. Cho, H. W. Kang, J. H. Seo, C. Jeon and K. B. Yoon, *Angew. Chem., Int. Ed.*, 2015, **54**, 13080–13084.
43 T. Mahdi and D. W. Stephan, *Angew. Chem., Int. Ed.*, 2015, **54**, 8511–8514.
44 M. Trunk, J. F. Teichert and A. Thomas, *J. Am. Chem. Soc.*, 2017, **139**, 3615–3618.
45 M. Murdoch, G. I. N. Waterhouse, M. A. Nadeem, J. B. Metson, M. A. Keane, R. F. Howe, J. Llorca and H. Idriss, *Nat. Chem.*, 2011, **3**, 489–492.
46 J. L. Fiorio, N. López and L. M. Rossi, *ACS Catal.*, 2017, **7**, 2973–2980.
47 W. J. Wang, M. Zhou and D. Q. Yuan, *J. Mater. Chem. A*, 2017, **5**, 1334–1347.
48 D. H. Deng, K. S. Novoselov, Q. Fu, N. F. Zheng, Z. Q. Tian and X. H. Bao, *Nat. Nanotechnol.*, 2016, **11**, 218–230.
49 Y. B. Huang, J. Liang, X. S. Wang and R. Cao, *Chem. Soc. Rev.*, 2017, **46**, 126–157.
50 A. M. Zheng, S. H. Li, S. B. Liu and F. Deng, *Acc. Chem. Res.*, 2016, **49**, 655–663.